THE JOURNAL OF PHYSICAL CHEMISTRY B

Article

pubs.acs.org/JPCB

Simulation of Two-Dimensional Electronic Spectra of Phycoerythrin 545 at Ambient Temperature

Xuan Leng and Xian-Ting Liang*

Department of Physics and Institute of Optics, Ningbo University, Ningbo 315211, China

ABSTRACT: By using a hierarchical equations-of-motion approach, we reproduce the two-dimensional electronic spectra of phycoerythrin 545 from *Rhodomonas* CS24 at ambient temperature (294 K). The simulated spectra are in agreement with the experimental results reported in Wong et al. (*Nat. Chem.* **2012**, *4*, 396). The evolutions of cross peaks for rephasing spectra and diagonal peaks for nonrephasing spectra have also been plotted. The peaks oscillate with the population times, with frequencies, phases, and amplitudes of the oscillating curves also being qualitatively consistent with the experimental results.

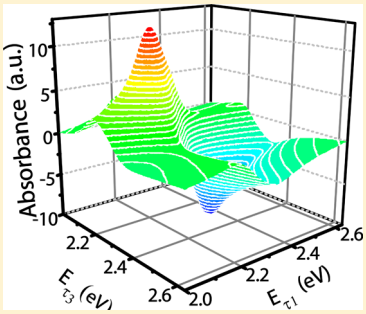

INTRODUCTION

Cryptophytes are eukaryotic algae that live in marine and freshwater environments. Their light-harvesting antenna proteins (phycobiliproteins) exhibit exceptional spectral variation, and they can photosynthesize in low-light conditions. The interchromophore separations in cryptophytes are much larger than in another light-harvesting system, Fenna-Matthews-Olson (FMO). The average nearest-neighbor center-to-center separation of chromophores within the cryptophyte light-harvesting antenna proteins is ∼20 Å.[1]

Collini et al. experimentally investigated the two-dimensional (2D) electronic spectra (ES) of phycoerythrin 545 (PE545) from *Rhodomonas* CS24[2] using photon-echo experiments. They showed that exceptionally long lasting quantum coherence exists in energy transfer processes in PE545 even at ambient temperature. This suggests that distant molecules within the light-harvesting protein are "wired" together by quantum coherence for a longer time, explaining the efficient energy transfer in cryptophyte marine algae. More recently, Wong et al. studied the excitonic correlations in PE545 by using a 2D ES method.[3]

Theoretically, Novoderezhkin et al.[4] investigated the excitation dynamics in PE545 by modeling the steady-state spectra and transient absorption using the modified Redfield theory. Using quantum-mechanics/molecule mechanics (QM/MM), Curutchet et al. investigated the energy transfer dynamics in the PE545 complex.[5] Viani et al. investigated the spatial and electronic correlation in the complex by using the QM/MM method.[6] These theoretical investigations suggest that there is coherence between different states in the light-harvesting complex, and this may enhance the efficiency of energy transfer in this light-harvesting system.

Two-dimensional ES is a powerful tool for probing the dynamics and constructions of complex biosystems. Reproducing experimental 2D ES is important for understanding the energy transfer mechanism in light-harvesting systems. However, until now, experimental 2D ES for PE545 have not been reproduced by using theoretical simulations. In this paper, we shall use the model Hamiltonian of PE545 and a nonperturbative, non-Markovian dynamics hierarchical equations-of-motion (HEM) approach to calculate the 2D ES of this kind of complex. Our simulation results will be compared with the experimental ones.

Mukamel and co-workers founded the theoretical framework of multidimensional nonlinear spectroscopy.[7] As is known, simulations of 2D ES are based on dynamical solutions for quantum dissipative systems. For systems such as the PE545 complex, there is no exact approach to solve its dynamics. Therefore, many approximation methods have been developed to calculate the 2D ES. The cumulant expansion method based on standard perturbation theory was first introduced by Makamel et al.[7,8] for calculating the nonlinear response functions. Later, the master equations of Redfield form,[9,10] and modified Redfield form[11,12] were used to calculate the response functions. Since then, significant progress has been achieved in simulating the 2D ES. However, these methods are totally or partly based on the Markovian approximation; therefore, total or partial memory effects of the environment have been excluded when we use these dynamical methods. However, it has been noted that environmental memory effects should not be ignored in the investigation of biosystems. Consequently, several non-Markovian approaches have been introduced recently for calculating the 2D ES.[13−23]

The HEM is an exact numerically dynamical method and it is nonperturbative and non-Markovian. It has already been successfully used to model excitonic energy transfer (EET) in pigment protein aggregates,[17,24] as well as to simulate the 2D ES of the FMO complex.[25,26] It has been compared to the

Received: July 13, 2014
Revised: October 8, 2014
Published: October 9, 2014

Table 1. Elements of the PE545 Hamiltonian (cm^{-1})

	DBV_{19A}	DBV_{19B}	PEB_{158C}	PEB_{158D}	$PEB_{50/61C}$	$PEB_{50/61D}$	PEB_{82C}	PEB_{82D}
DBV_{19A}	18008	−4.1	−31.9	2.8	2.1	−37.1	−10.5	45.9
DBV_{19B}	−4.1	17973	−2.9	30.9	−35.4	2.5	−45.5	11.0
PEB_{158C}	−31.9	−2.9	18711	−5.6	−19.6	−16.1	6.7	6.8
PEB_{158D}	2.8	30.9	−5.6	18960	11.5	25.5	5.1	7.4
$PEB_{50/61C}$	2.1	−35.4	−19.6	11.5	18532	101.5	36.3	16.0
$PEB_{50/61D}$	−37.1	2.5	−16.1	25.5	101.5	19574	17.6	−38.6
PEB_{82C}	−10.5	−45.5	6.7	5.1	36.3	17.6	18040	2.6
PEB_{82D}	45.9	11.0	6.8	7.4	16.0	−38.6	2.6	19050

Poisson mapping bracket equation (PBME) in the investigation of the EET for another light-harvesting system, PC645,[27] in which the HEM method shows more sophisticated changes of density matrix elements than the PBME. Fassioli et al. discussed coherent energy transfer under incoherent light conditions in PC645 by using the HEM approach.[28] They noted that the light-harvesting antenna has mechanisms that could support coherent evolution under incoherent illumination. The HEM method is an effective dynamical approach and is suitable for simulating the 2D ES of PE545, and, in fact, it has been applied to investigations of 2D ES of other systems.[25,26,29−31]

In this paper, we calculate the 2D ES of PE545. It will be shown that the major signatures of the experimental 2D ES can be reproduced in our theoretical simulations. This suggests that this theoretical method holds promise for investigating the 2D ES of some complex light-harvesting systems and that the model Hamiltonian has captured the major characteristics of the system. Differences between theoretical and experimental results may also guide the direction of improvements in the model and dynamical method.

MODEL AND METHOD

Within this theoretical framework, PE545 is described by using a Frankel exciton model, and the total Hamiltonian of the open system can be written as

$$H = H_S + H_B + H_{SB} \tag{1}$$

where H_S describes the exciton system, the environment is modeled with an infinite set of harmonic vibrations $H_B = \sum_m \hbar\omega_m b_m^\dagger b_m$, and H_{SB} is the coupling term between the system and its environment.[24−26,30] The elements of the exciton Hamiltonian for PE545 are listed in Table 1.[32] Here, the diagonal terms are the site energies (transition energies) of the exciton model, and the off-diagonal terms describe the interactions (electronic couplings) between different sites.

The linear absorption spectrum is given by the Fourier transform of the autocorrelation function of the transition dipole moment (TDM) operator $\boldsymbol{\mu}$:[33]

$$I(\omega) = \mathrm{Re}\int_0^\infty e^{i\omega}\langle \boldsymbol{\mu}(t)\boldsymbol{\mu}(0)\rangle_g \tag{2}$$

where $\boldsymbol{\mu}(t) = e^{iHt/\hbar}\boldsymbol{\mu}e^{-iHt/\hbar}$ is the TDM operator in the Heisenberg picture, $\boldsymbol{\mu} = \sum_m \boldsymbol{\mu}_m(|m\rangle\langle 0| + |0\rangle\langle m|)$, and $\boldsymbol{\mu}_m$ is the TDM operator of site m. The subscript g indicates that the initial state to calculate the autocorrelation function is equilibrated on the ground electronic state, $\rho_g = |0\rangle\langle 0| \otimes e^{-\beta H_B}/\mathrm{Tr}\, e^{-\beta H_B}$, where $\beta = 1/K_B T$ with Boltzmann constant K_B and temperature T. The values of the transition dipole moments ($\boldsymbol{\mu}_m$ values) and their components μ_{mx}, μ_{my}, and μ_{mz} are given in Table 2 (see also ref 34).

Table 2. Transition Dipole Moments $\boldsymbol{\mu}_m$ and Their Components μ_{mx}, μ_{my}, and μ_{mz} for Each of the Eight Pigments of PE545

pigment (m)	μ_{mx}	μ_{my}	μ_{mz}	$\boldsymbol{\mu}_m$
DBV_{19A}	−4.506	−2.670	0.200	13.32
DBV_{19B}	5.102	0.280	1.574	13.59
PEB_{158C}	0.448	−0.873	4.691	12.18
PEB_{158D}	1.383	−4.355	−1.445	12.18
$PEB_{50/61C}$	−0.088	−2.605	−4.019	12.17
$PEB_{50/61D}$	0.216	2.422	3.992	11.87
PEB_{82C}	2.898	1.310	−3.721	12.44
PEB_{82D}	−3.900	2.600	1.258	12.33

The 2D ES can be calculated through the third-order optical response function, which is[26,30]

$$S^{(3)}(\tau_3, \tau_2, \tau_1) = \left(\frac{i}{\hbar}\right)^3 \mathrm{Tr}\{\mu(\tau_3 + \tau_2 + \tau_1)[\mu(\tau_2 + \tau_1), [\mu(\tau_1), [\mu, \rho_g]]]\} \tag{3}$$

By applying the rotating-wave approximation and phase matching, the response functions of the rephasing and nonrephasing signals become

$$S_{rp}(\tau_3, \tau_2, \tau_1) \equiv \mathrm{Tr}\{\mu_- \hat{G}(\tau_3)\mu_+^\times \hat{G}(\tau_2)\mu_+^\times \hat{G}(\tau_1)\mu_-^\times \rho_g\} \tag{4}$$

$$S_{nr}(\tau_3, \tau_2, \tau_1) \equiv \mathrm{Tr}\{\mu_- \hat{G}(\tau_3)\mu_+^\times \hat{G}(\tau_2)\mu_-^\times \hat{G}(\tau_1)\mu_+^\times \rho_g\} \tag{5}$$

Here, $G(\tau)$ is the retarded propagator of the total system in the Liouville space; $\tau_1 = t_2 - t_1$, $\tau_2 = t_3 - t_2$, and $\tau_3 = t - t_3$, with time points t_1, t_2, and t_3 of the laser projecting to the sample; and $\mu_- = \sum \mu_m|g\rangle\langle m|$, $\mu_+ = \sum \mu_m|m\rangle\langle g|$, and $\mu_\pm^\times A = \mu_\pm A - A\mu_\pm$. In the impulsive limit, the 2D rephasing (rp), nonrephasing (nr), and purely absorptive (ab) 2D ES can be calculated with

$$I_{\mathrm{rp}}(\omega_3, \tau_2, \omega_1) = \mathrm{Re}\int_0^\infty d\tau_1 \int_0^\infty d\tau_3 e^{i(-\omega_1\tau_1 + \omega_3\tau_3)} S_{\mathrm{rp}}(\tau_3, \tau_2, \tau_1) \tag{6}$$

$$I_{\mathrm{nr}}(\omega_3, \tau_2, \omega_1) = \mathrm{Re}\int_0^\infty d\tau_1 \int_0^\infty d\tau_3 e^{i(-\omega_1\tau_1 + \omega_3\tau_3)} S_{\mathrm{nr}}(\tau_3, \tau_2, \tau_1) \tag{7}$$

$$I_{\mathrm{ab}}(\omega_3, \tau_2, \omega_1) = I_{\mathrm{rp}}(\omega_3, \tau_2, -\omega_1) + I_{\mathrm{nr}}(\omega_3, \tau_2, \omega_1) \tag{8}$$

The HEM scheme can be used to calculate eq 4, where we set $C_1(\tau_1) = \hat{G}(\tau_1)[\mu_-^\times \rho_g]$ in $\tau_1(t_1 \to t_2)$, $C_2(\tau_2, \tau_1) = \hat{G}(\tau_2)[\mu_+^\times C_1(\tau_1)]$ in $\tau_2(t_2 \to t_3)$, $C_3(\tau_3, \tau_2, \tau_1) = \hat{G}(\tau_3)$-$[\mu_+^\times C_2(\tau_2, \tau_1)]$ in $\tau_3(t_3 \to t)$, and finally $S_{\mathrm{rp}}(\tau_3, \tau_2, \tau_1) = \mathrm{Tr}[\mu_- C_3(\tau_1, \tau_2, \tau_3)]$. Similarly, we can calculate eq 5, $S_{\mathrm{nr}}(\tau_3, \tau_2, \tau_1)$.

dx.doi.org/10.1021/jp506974r | J. Phys. Chem. B 2014, 118, 12366−12370

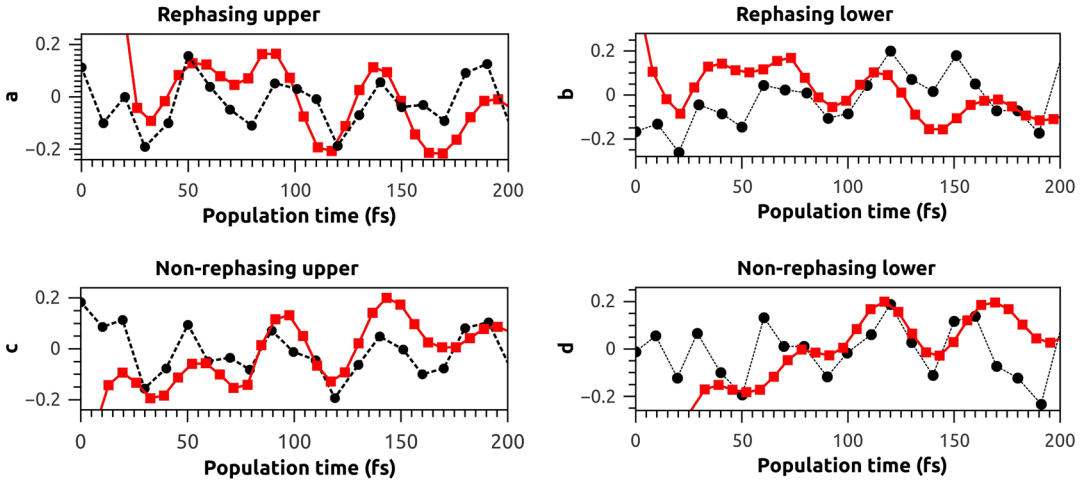

Figure 1. Oscillations of real rephasing ES at cross peaks (a) (2.18, 2.26) eV and (b) (2.26, 2.18) eV and real nonrephasing ES at diagonal peaks (c) (2.26, 2.26) eV and (d) (2.18, 2.18) eV. The red squares are our calculation results, and the black circles are results extracted from ref 3.

In fact, the scheme employed here is the same as that used for the calculation of the reduced density matrix $\rho(t) = \mathrm{Tr}_{Bath}[\hat{G}(\tau)\rho(0)]$ with the HEM approach, which describes the evolution of a set of auxiliary density operators ρ_n, namely,[17,24,25]

$$\frac{\mathrm{d}}{\mathrm{d}t}\rho_n = -\frac{i}{\hbar}[H_S, \rho_n] - \gamma\sum_{m=1}^{N} n_m\rho_n - \sum_{m=1}^{N}\left[\frac{2\lambda}{\beta\gamma\hbar^2} - \frac{\lambda}{\hbar}\cot\left(\frac{\beta\gamma\hbar}{2}\right)\right]\times|m\rangle\langle m|, [|m\rangle\langle m|, \rho_n]] - i\sum_{m=1}^{N}[|m\rangle\langle m|, \rho_{n_m^+}] - \frac{i}{\hbar}\sum_{m=1}^{N} n_m(c_0|m\rangle\langle m|\rho_{n_m^-} - c_0^*\rho_{n_m^-}|m\rangle\langle m|) \quad (9)$$

where $c_0 = \lambda\gamma[\cot(\beta\gamma\hbar/2) - i]$, and the Drude−Lorentz spectra $J(\omega) = 2\lambda\gamma\omega/(\omega^2 + \gamma^2)$ are used. λ and γ are the reorganization energy and cutoff frequency of the investigated system, respectively. In this paper, we set $\lambda = 150\ \mathrm{cm}^{-1}$ and $\gamma^{-1} = 60$ fs according to ref 28. The subscript $\boldsymbol{n}$ denotes the set of indices $\boldsymbol{n} = (n_1, n_2, ..., n_N)$, and $\boldsymbol{n}_m^{\pm}$ differs from $\boldsymbol{n}$ only by changing the specified n_m to $n_m \pm 1$. Particularly, ρ_0 with $\mathbf{0} = (0, 0, ..., 0)$ is the system-reduced density operator, while the other ρ_n values are the auxiliary density operators. We truncate the hierarchy at $L = \sum_{m=1}^{N} n_m = 3$ in this paper. It is worth noting that the low-temperature correction terms are added in eq 9,[17,24,26] and therefore, it is sufficiently exact for our calculations at ambient temperature (294 K). In addition, the disorder of the diagonal terms of the Hamiltonian are considered, and that of the off-diagonal terms are neglected, when we calculate the 2D ES. Each plot in our work is obtained by averaging over 100 samples with a Gaussian distribution, and their standard deviation is set to $\sigma = 400\ \mathrm{cm}^{-1}$.[34] The rotational averages[26] are also taken into account in our calculations; namely, we choose 100 random directions for calculating each plot.

RESULTS AND DISCUSSION

In ref 3, two kinds of cases are investigated. The first one is that for a laser with relatively narrow excitation bandwidth compared to the linear absorption spectrum of PE545. Thus, only parts of the sites are excited and their responses are probed in the photon-echo experiments. In ref 3 the authors attempted to use many kinds of lasers with different bandwidths, and the so-called "red excitation conditions" in which the bandwidth overlaps DBV_{19B}, DBV_{19A}, PEB_{82C}, $\mathrm{PEB}_{50/61C}$, and PEB_{158C} have been investigated in detail. The second case is that for laser pulses with relatively broader excitation bandwidth that can overlap the majority of the linear absorption spectrum for PE545. In this case, all PE545 sites are excited and probed in the photon-echo experiments. In the following, we numerically investigate the 2D ES corresponding to these two kinds of cases.

First, we study the red excitation conditions model defined in ref 3. In this case, the evolutions of a pair cross peaks, (2.18, 2.26) and (2.26, 2.18) eV, of rephasing signals and a pair of diagonal peaks, (2.18, 2.18) and (2.26, 2.26) eV, of non-rephasing signals with the population times are calculated. In Figure 1, we plot the evolutions of the amplitudes of the cross peaks of the rephasing ES (left) and of the diagonal peaks of the nonrephasing ES (right) with the population times. The red squares are our calculation results, and the black circles are extracted from Figure 1e of ref 3. One can see that the calculation data have clearly shown the signatures exhibited by the experimental data. For example, the amplitudes of the cross peaks of the rephasing ES and the diagonal peaks of the nonrephasing ES are oscillating with the population times, and these oscillations are directly related to the phase evolutions of off-diagonal elements in the density matrix, which means that the system is a coherent superposition of states during its evolution.[35] Further, we note that the oscillations of the amplitudes with the population times for the cross peaks (2.18, 2.26) and (2.26, 2.18) eV in the rephasing ES and those for the diagonal peaks (2.18, 2.18) and (2.26, 2.26) eV in the nonrephasing ES are phase reversed. The oscillation frequencies are in agreement with the formula $2\pi(E_a - E_b)/\hbar$, where E_a and E_b are the site energies of the coupled sites. However, the theoretical data do not conform perfectly to the experimental results, although they have similar oscillating signatures; therefore, additional work needs to be carried out to understand the energy transfer within the complex.

We next investigate the second case. Namely, we reproduce the 2D ES of Figure 2 in ref 3. Here, all sites of PE545 are excited. Figure 2a shows the linear absorption spectrum of

dx.doi.org/10.1021/jp506974r | J. Phys. Chem. B 2014, 118, 12366−12370

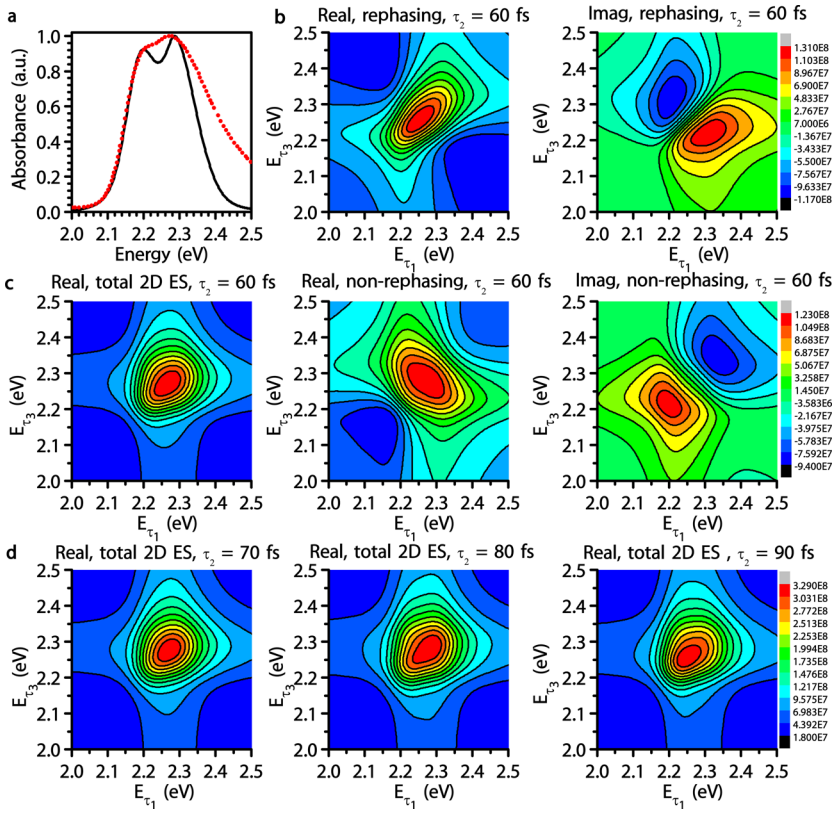

Figure 2. (a) Linear absorption spectrum of PE545 through simulation (black lines) and experimental measurement (red dots). (b) Real (left) and imaginary (right) components of the rephasing (upper) and nonrephasing (lower) ES at population time τ_2 = 60 fs. (c and d) Real purely absorptive 2D ES at population times τ_2 = 60, 70, 80, 90 fs, respectively. Here, the simulation parameters are λ = 150 cm^{-1} and γ^{-1} = 60 fs, and the temperature is 294 K.

PE545; the red dots are extracted from Figure 2a in ref 3, and the black line is calculated by using our model. One can see that our simulation data are quite consistent with the experimental ones except at higher energies. The four panels of Figure 2b (upper right) show simulations of the 2D ES of real (left) rephasing (upper) and imaginary (right) nonrephasing (lower) spectra at the population time τ_2 = 60 fs. The positions, forms, and scales of the cross and diagonal peaks are seen to be all similar to the experimental spectra, shown in Figure 2 in ref 3. Parts c and d (the lowest three panels) of Figure 2c show plots of the purely absorptive 2D ES at the population times τ_2 = 60, 70, 80, and 90 fs. The forms, positions, and scales of the peaks in frequency space are similar to the corresponding spectra in ref 3. However, there are some differences between the theoretical and experimental results: (1) The linear absorption spectra (see Figure 2a) of our simulation and the experiment have some differences at higher energy. (2) The purely absorptive 2D ES of our simulations (see Figure 2, parts c and d) have a little deformation compared to the experimental ones (see Figure 2c,d in ref 3). These differences suggest that our model (including an environmental model and/or a dynamical method) should be improved further to exactly describe the 2D ES. This may prove to be a meaningful research direction for investigating energy transfer in light-harvesting complexes.

CONCLUSION

In conclusion, in this paper, we reproduced the 2D ES of PE545 from *Rhodomonas* CS24 at ambient temperature (294 K). It was shown that the evolutions of the cross peaks for the rephasing ES and the diagonal peaks for the nonrephasing ES and purely absorptive 2D ES are oscillating with the population times. In particular, our theoretical simulations showed that the oscillations for the cross peaks (2.18, 2.26) and (2.26, 2.18) eV of the rephasing signals and the diagonal peaks (2.18, 2.18) and (2.26, 2.26) eV of the nonrephasing signals are phase reversed, which is in agreement with the experimental data. The oscillating frequencies, amplitudes, and peak positions were also found to be similar to the experimental results. The 2D ES signals at electronic cross peaks indicate that transitions of electrons at one site of PE545 influence those at others. The oscillations of the cross peaks imply that the electrons are in coherent superposition states during the transition process. The quantitative agreement of some important signatures of the theoretical and measured 2D ES for PE545 means that the long-lasting coherence can be understood within the framework of quantum mechanics. This may help us identify probable connections between quantum effects and efficient energy transfer in light-harvesting complexes in the future.

AUTHOR INFORMATION

Corresponding Author

*E-mail: liangxianting@nbu.edu.cn.

Notes

The authors declare no competing financial interest.

ACKNOWLEDGMENTS

This project was sponsored by the National Natural Science Foundation of China (Grant No. 61078065), the Zhejiang Provincial Natural Science Foundation of China (Grant No.

LY13A040006), and the K. C. Wong Magna Foundation at Ningbo University.

REFERENCES

(1) Wilk, K. E.; Harrop, S. J.; Jankova, L.; Edler, D.; Keenan, G.; Sharples, F.; Hiller, R. G.; Curmi, P. M. Evolution of a light-harvesting protein by addition of new subunits and rearrangement of conserved elements: Crystal structure of a cryptophyte phycoerythrin at 1.63-Å resolution. *Proc. Natl. Acad. Sci. U.S.A.* **1999**, *96*, 8901−8906.

(2) Collini, E.; Wong, C. Y.; Wilk, K. E.; Curmi, P. M.; Brumer, P.; Scholes, G. D. Coherently wired light-harvesting in photosynthetic marine algae at ambient temperature. *Nature* **2010**, *463*, 644−647.

(3) Wong, C. Y.; Alvey, R. M.; Turner, D. B.; Wilk, K. E.; Bryant, D. A.; Curmi, P. M.; Silbey, R. J.; Scholes, G. D. Electronic coherence lineshapes reveal hidden excitonic correlations in photosynthetic light harvesting. *Nat. Chem.* **2012**, *4*, 396−404.

(4) Novoderezhkin, V. I.; Doust, A. B.; Curutchet, C.; Scholes, G. D.; van Grondelle, R. Excitation dynamics in phycoerythrin 545: modeling of steady-state spectra and transient absorption with modified Redfield theory. *Biophys. J.* **2010**, *99*, 344−352.

(5) Curutchet, C.; Novoderezhkin, V. I.; Kongsted, J.; Munoz-Losa, A.; van Grondelle, R.; Scholes, G. D.; Mennucci, B. Energy flow in the cryptophyte PE545 antenna is directed by bilin pigment conformation. *J. Phys. Chem. B* **2013**, *117*, 4263−4273.

(6) Viani, L.; Curutchet, C.; Mennucci, B. Spatial and Electronic Correlations in the PE545 Light-Harvesting Complex. *J. Phys. Chem. Lett.* **2013**, *4*, 372−377.

(7) Mukamel, S. *Principles of nonlinear optical spectroscopy*; Oxford University Press: New York, NY, 1995; Vol. *29*.

(8) Mukamel, S. Multidimensional femtosecond correlation spectroscopies of electronic and vibrational excitations. *Annu. Rev. Phys. Chem.* **2000**, *51*, 691−729.

(9) Mančal, T.; Pisliakov, A. V.; Fleming, G. R. Two-dimensional optical three-pulse photon echo spectroscopy. I. Nonperturbative approach to the calculation of spectra. *J. Chem. Phys.* **2006**, *124*, 234504.

(10) Pisliakov, A. V.; Mančal, T.; Fleming, G. R. Two-dimensional optical three-pulse photon echo spectroscopy. II. Signatures of coherent electronic motion and exciton population transfer in dimer two-dimensional spectra. *J. Chem. Phys.* **2006**, *124*, 234505.

(11) Zhang, W. M.; Meier, T.; Chernyak, V.; Mukamel, S. Exciton-migration and three-pulse femtosecond optical spectroscopies of photosynthetic antenna complexes. *J. Chem. Phys.* **1998**, *108*, 7763−7774.

(12) Mukamel, S.; Abramavicius, D. Many-body approaches for simulating coherent nonlinear spectroscopies of electronic and vibrational excitons. *Chem. Rev.* **2004**, *104*, 2073−2098.

(13) Tanimura, Y.; Kubo, R. Two-time correlation functions of a system coupled to a heat bath with a Gaussian-Markoffian interaction. *J. Phys. Soc. Jpn.* **1989**, *58*, 1199−1206.

(14) Tanimura, Y. Nonperturbative expansion method for a quantum system coupled to a harmonic-oscillator bath. *Phys. Rev. A* **1990**, *41*, 6676.

(15) Tanimura, Y. Stochastic Liouville, Langevin, Fokker-Planck, and master equation approaches to quantum dissipative systems. *J. Phys. Soc. Jpn.* **2006**, *75*.

(16) Ishizaki, A.; Tanimura, Y. Quantum dynamics of system strongly coupled to low-temperature colored noise bath: reduced hierarchy equations approach. *J. Phys. Soc. Jpn.* **2005**, *74*, 3131−3134.

(17) Ishizaki, A.; Fleming, G. R. Theoretical examination of quantum coherence in a photosynthetic system at physiological temperature. *Proc. Natl. Acad. Sci. U.S.A.* **2009**, *106*, 17255−17260.

(18) Xu, R.-X.; Cui, P.; Li, X.-Q.; Mo, Y.; Yan, Y. Exact quantum master equation via the calculus on path integrals. *J. Chem. Phys.* **2005**, *122*, 041103.

(19) Yan, Y.; Xu, R. Quantum mechanics of dissipative systems. *Annu. Rev. Phys. Chem.* **2005**, *56*, 187−219.

(20) Xu, R.-X.; Yan, Y. Dynamics of quantum dissipation systems interacting with bosonic canonical bath: Hierarchical equations of motion approach. *Phys. Rev. E* **2007**, *75*, 031107.

(21) Xu, R.-X.; Tian, B.-L.; Xu, J.; Yan, Y. Exact dynamics of driven Brownian oscillators. *J. Chem. Phys.* **2009**, *130*, 074107.

(22) Sahrapour, M. M.; Makri, N. Multitime response functions and nonlinear spectra for model quantum dissipative systems. *J. Chem. Phys.* **2010**, *132*, 134506.

(23) Liang, X.-T. Simulating signatures of two-dimensional electronic spectra of the Fenna-Matthews-Olson complex: By using a numerical path integral. *J. Chem. Phys.* **2014**, *141*, 044116.

(24) Strumpfer, J.; Schulten, K. Open Quantum Dynamics Calculations with the Hierarchy Equations of Motion on Parallel Computers. *J. Chem. Theory Comput.* **2012**, *8*, 2808−2816.

(25) Chen, L.; Zheng, R.; Jing, Y.; Shi, Q. Simulation of the two-dimensional electronic spectra of the Fenna-Matthews-Olson complex using the hierarchical equations of motion method. *J. Chem. Phys.* **2011**, *134*, 194508.

(26) Hein, B.; Kreisbeck, C.; Kramer, T.; Rodriguez, M. Modelling of oscillations in two-dimensional echo-spectra of the Fenna-Matthews-Olson complex. *New J. Phys.* **2012**, *14*, 023018.

(27) Lee, W.-G.; Rhee, Y. M. Excitonic Energy Transfer of Cryptophyte Phycocyanin 645 Complex in Physiological Temperature by Reduced Hierarchical Equation of Motion. *Bull. Korean Chem. Soc.* **2014**, *35*, 859.

(28) Fassioli, F.; Olaya-Castro, A.; Scholes, G. D. Coherent energy transfer under incoherent light conditions. *J. Phys. Chem. Lett.* **2012**, *3*, 3136−3142.

(29) Ishizaki, A.; Tanimura, Y. Nonperturbative non-Markovian quantum master equation: Validity and limitation to calculate nonlinear response functions. *Chem. Phys.* **2008**, *347*, 185−193.

(30) Chen, L.; Zheng, R.; Shi, Q.; Yan, Y. Two-dimensional electronic spectra from the hierarchical equations of motion method: Application to model dimers. *J. Chem. Phys.* **2010**, *132*, 024505.

(31) Zhang, P.-P.; Liu, Z.-Q.; Liang, X.-T. Two-dimensional electronic spectra investigated using hierarchical equation of motion and cumulant expansion. *J. Mod. Opt.* **2013**, *60*, 301−308.

(32) Hossein-Nejad, H.; Curutchet, C.; Kubica, A.; Scholes, G. D. Delocalization-enhanced long-range energy transfer between cryptophyte algae PE545 antenna proteins. *J. Phys. Chem. B* **2011**, *115*, 5243−5253.

(33) Chen, L.; Zheng, R.; Shi, Q.; Yan, Y. Optical line shapes of molecular aggregates: Hierarchical equations of motion method. *J. Chem. Phys.* **2009**, *131*, 094502.

(34) Novoderezhkin, V. I.; Doust, A. B.; Curutchet, C.; Scholes, G. D.; van Grondelle, R. Excitation dynamics in phycoerythrin 545: modeling of steady-state spectra and transient absorption with modified Redfield theory. *Biophys. J.* **2010**, *99*, 344−352.

(35) Braczyk, A. M.; Turner, D. B.; Scholes, G. D. Crossing disciplines - A view on two-dimensional optical spectroscopy. *Ann. Phys.* **2014**, *526*, 31−49.